Mol. Cells *27*, 667-671, June 30, 2009
DOI/10.1007/s10059-009-0088-x

Molecules and Cells

Crystal Structure of *Rattus norvegicus* Visfatin/PBEF/Nampt in Complex with an FK866-Based Inhibitor

Gil Bu Kang[1,2,3], Man-Ho Bae[1,2,3], Mun-Kyoung Kim[1], Isak Im[1], Yong-Chul Kim[1], and Soo Hyun Eom[1,2,*]

Visfatin (Nampt/PBEF) plays a pivotal role in the salvage pathway for NAD^+ biosynthesis. Its potent inhibitor, FK866, causes cellular NAD^+ levels to decline, thereby inducing apoptosis in tumor cells. In an effort to improve the solubility and binding interactions of FK866, we designed and synthesized IS001, in which a ribose group is attached to the FK866 pyridyl ring. Here, we report the crystal structure of rat visfatin in complex with IS001. Like FK866, IS001 is positioned at the dimer interface, and all of the residues that interact with IS001 are involved in hydrophobic or π-π-stacking interactions. However, we were unable to detect any strong interactions between the added ribose ring of IS001 and visfatin, which implies that a bulkier modifying group is necessary for a tight interaction. This study provides additional structure-based information needed to optimize the design of visfatin inhibitors.

INTRODUCTION

Nicotinamide adenine dinucleotide (NAD^+) plays a pivotal role in a variety biochemical and biological processes, serving both as an enzyme cofactor for oxidation/reduction and as a substrate for donation of ADP-ribose units (Won et al., 2006; Ziegler et al., 2000). Notably, malignant tumor cells show higher than normal rates of NAD^+ turnover, owing to their elevated ADP-ribosylation activity (Burkle, 2005; Schreiber et al., 2006). Moreover, expression of visfatin [pre-B-cell colony-enhancing factor (PBEF)/nicotinamide phosphoribosyltransferase (Nampt)], the rate-limiting enzyme in the salvage pathway for NAD^+ synthesis, is upregulated in malignant tumor cells, so as to maintain adequate levels of NAD^+ (Hufton et al., 1999; Van Beijnum et al., 2002). This makes visfatin an attractive target for anticancer therapy (Wosikowski et al., 2002).

FK866 (APO866; (E)-N-[4-(1-benzoylpiperidin-4-yl) butyl]-3-(pyridin-3-yl) acrylamide) is a potent small-molecule inhibitor of visfatin that induces apoptosis among tumor cells as a consequence of reducing NAD^+ levels (Hasmann and Shcemainda, 2003). It also has been shown to have anti-angiogenic effects in a murine cancer model (Drevs et al., 2003). A phase I clinical trial of FK866 has already been successfully completed (Holen et al., 2008), and a phase II trial of its efficacy against several forms of human cancer is currently ongoing. Nevertheless, preclinical pharmacology showed the low bioavailability and rapid intravenous clearance of FK866 (Holen et al., 2008), indicating that it should be further optimized for therapeutic usage.

The crystal structures of visfatin in complex with FK866 or nicotinamide mononucleotide (NMN) have already been described (Khan et al., 2006; Kim et al., 2006; Wang et al., 2006). The structure of the visfatin-FK866 complex reveals how the inhibitor interacts with the enzyme's active site residues, while comparison of the structures of the visfatin-FK866 and visfatin-NMN complexes shows how the pyridyl ring of FK866 is positioned at the nicotinamide ring of NMN. Given that the ribose ring and phosphate group of NMN make good contact with the active site residues of visfatin, we endeavored to design a larger FK866 derivative that would establish hydrogen bond interactions with residues in the NMN binding site.

Toward that goal, we designed several hydrophilic moieties, which we added to FK866 in an effort to manipulate its solubility and binding interactions. Ultimately, we designed and synthesized IS001, in which a ribose ring was added to the FK866 pyridyl ring. Then to better understand the molecular mechanism underlying the visfatin-IS001 interaction, we determined the crystal structure of the visfatin-IS001 complex and used isothermal titration calorimetry (ITC) to assess the affinity of IS001 for visfatin.

MATERIALS AND METHODS

Protein expression and purification

The overexpression of rat visfatin and its purification have been described previously (Kim et al., 2006). Briefly, a recombinant rat visfatin-His-tag fusion protein was expressed in *E. coli* BL21 (DE3) at 37°C, after which the cell lysate was applied to a Ni-NTA affinity chromatography column. The column was then washed with lysis buffer [500 mM NaCl and 50 mM NaH_2PO_4 (pH 8.0)], the recombinant visfatin-His-tag fusion protein was

[1]Department of Life Science, Gwangju Institute of Science and Technology, Gwangju 500-712, Korea, [2]Cell Dynamics Research Center and Research Center for Biomolecular Nanotechnology, Gwangju Institute of Science and Technology, Gwangju 500-712, Korea, [3]These authors contributed equally to this work.
*Correspondence: eom@gist.ac.kr

Received February 13, 2009; revised April 16, 2009; accepted April 17, 2009; published online June 12, 2009

Keywords: crystal structure, FK866, nicotinamide phosphoribosyltransferase (Nampt), pre-B-cell colony-enhancing factor (PBEF), visfatin

eluted using a buffer [300 mM imidazole, 500 mM NaCl and 50 mM NaH_2PO_4 (pH 8.0)], and the N-terminal His-tag was removed by digestion with TEV protease. The protein was then subjected to size exclusion chromatography on a Superdex 200 column (Pharmacia) equilibrated with 20 mM HEPES-NaOH (pH 7.5) and 150 mM NaCl. Fractions containing the recombinant protein were pooled and concentrated to 15 mg/ml.

Isothermal titration calorimetry experiments

IS001 was synthesized by ribosylation of the FK866 pyridyl ring using β-D-ribofuranose 1,2,3,4-tetraacetate (to be published). ITC was then carried out using a high-precision VP-ITC titration calorimetry instrument (Microcal Inc., USA) with human visfatin and IS001. The binding enthalpies were determined by injecting IS001 into a microcalorimeter reaction cell containing human visfatin. In a typical ITC experiment, the heat of the reaction was determined by making 30 injections (10 μl each) of IS001 (final concentration in the syringe was 0.8 mM in 20 mM HEPES-NaOH and 150 mM NaCl) into the reaction cell, which contained 59 μM human visfatin in the same buffer. The heat after each injection was determined from the time integral of the calorimetric signal using Origin 7.0.

Crystallization

Crystallization of visfatin in complex with IS001 will be reported elsewhere (to be published). In brief, single well-formed crystals of rat visfatin in complex with IS001 were grown at 21°C in 2-μl hanging drops containing equal volumes of protein solution (15 mg/ml) and mother liquor comprised of 0.1 M HEPES-NaOH (pH 7.5), 16% (w/v) PEG 3350, and 0.2 M $MgCl_2$. Crystals were frozen in liquid nitrogen using paraton as a cryoprotectant.

Crystallographic analysis

The data set for the visfatin-IS001 complex was collected at beam line 4A at the Pohang Accelerator Laboratory (PAL), Korea using the X-ray beam at a single wavelength (1.0000 Å). Data processing and scaling were carried out using the program HKL2000 (Otwinowski and Minor, 1997). The crystals of rat visfatin in complex with IS001 diffracted to 3.0 Å resolution and belonged to space group $P2_12_12_1$ with cell parameters of a = 83.3 Å, b = 107.4 Å, and c = 120.2 Å. Assuming two molecules of rat visfatin-IS001 complex per asymmetric unit, the Matthews coefficient (V_M) was calculated to be 2.41 $Å^3 Da^{-1}$, which corresponds to a solvent content of 48.9%. The structure of the rat visfatin-IS001 complex was solved using the molecular replacement method with the program MOLREP (Vagin et al., 2000) using the apo-structure of rat visfatin (PDB ID: 2G95) as the search model. Many cycles of manual rebuilding using the program Coot (Emsley and Cowtan 2004) and refinement using the program CNS resulted in a final crystallographic R value of 25.4% (R_{free} = 29.7%). No electron density was observed in some regions of each molecule (residues 1-8, 42-53 and 484-491). The Ramachandran plot calculated with the program PROCHECK (Laskowski et al., 1993) showed no residues with torsional angles in forbidden areas: 75.9% of the residues were in the most favored regions and 24.1% were in allowed regions. Data collection and refinement statistics are summarized in Table 1. Atomic coordinates have been deposited at the Protein Data Bank under accession code 3G8E.

Table 1. Data collection and refinement statistics

Crystal	Visfatin-IS001 complex
X-ray source	PAL-4A
Wavelength (Å)	1.0000 Å
Space group	$P2_12_12_1$
Unit cell dimensions (Å)	a = 83.3, b = 107.4, c = 120.2
Resolution (Å)	50-3.0
Observed reflections	165,450
Unique reflections	22,256
Completeness (%)	99.7 (100)
R_{symm}[1] (%)	14.0 (33.4)
I/σ (I)	24.4 (8.3)
Refinement statistics	
Resolution (Å)	50-3.0 (3.05-3.00)
No. of Residues	926
[2]R_{cryst} total (%)	25.3
[3]R_{free} total (%)	29.9
[4]RMSD bond length (Å)	0.010
[4]RMSD bond angle (°)	1.8

Numbers in parentheses on the right side indicate the statistics for the last resolution shell.

[1]$R_{symm} = \Sigma_h\Sigma_i \mid I(h_i) - \langle I(h)\rangle \mid / \Sigma_h\Sigma_i I(h_i)$, where $I(h_i)$ is the single intensity of reflection h as determined by the ith measurement and $\langle I(h)\rangle$ is the mean intensity of reflections h.

[2]R_{cryst} (%) = $\Sigma \mid Fo - Fc \mid / \Sigma Fo$, where, Fo is the observed structure factor amplitude, and Fc is the structure factor calculated from the model.

[3]R_{free} (%) is calculated in the same manner as R_{cryst} using 5% of all reflections excluded from refinement stages.

[4]RMSD, Root-mean-square deviation.

RESULTS AND DISCUSSION

NAD^+ plays a critical role in a variety of cellular processes, including both redox and nonredox reactions. It also serves as an enzyme cofactor involved in energy metabolism and signal transduction. Proteins involved in NAD^+ synthesis are thus attractive targets for drug discovery. One such protein, visfatin, which is the rate-limiting enzyme in the salvage pathway for NAD^+ synthesis, is currently thought to be a highly attractive anticancer target.

FK866 is a potent and selective inhibitor of visfatin that interferes with NAD^+ biosynthesis, causing tumor cells to undergo apoptosis. For example, FK866 exhibits both anti-tumoral and anti-angiogenic activities in renal cell carcinoma, and effectively induces delayed apoptotic cell death in HepG2 human carcinoma cells. The structure of visfatin in complex with FK866 or NMN suggests that FK866 could be modified to take advantage of the binding sites on visfatin for NMN's ribose and phosphate groups. With that in mind, we designed and synthesized IS001, a derivative of FK866 in which a ribose was added to the pyridyl ring to enhance interactions with the ribose binding site on visfatin (Fig. 1). Then to investigate the molecular basis of the inhibitory effect of IS001, we determined the crystal structure of the rat visfatin-IS001 complex.

We found that the crystal structure of the rat visfatin-IS001 complex includes two monomers in the asymmetric unit, and that visfatin forms a homodimer comprised of two identical 491-residue subunits (Fig. 2). The structures of the visfatin-IS001 and visfatin-FK866 complexes are nearly identical. The root-mean-square deviation (RMSD) between the two structures is 0.52 Å for 926 C_α atoms, while the RMSD between the apo-structure and the IS001-complexed structure is 2.37 Å for 834

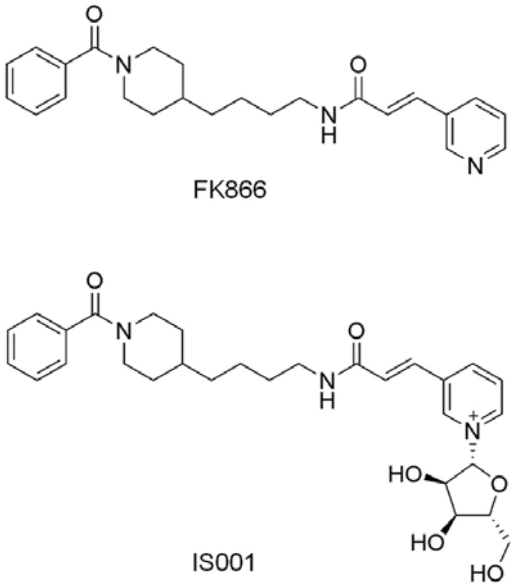

Fig. 1. Chemical structures of FK866 (A) and IS001 (B)

C_α atoms. Thus the structure of the visfatin-IS001 complex resembles that of the visfatin-FK866 complex more than the apo-structure.

The active site is located at the visfatin dimer interface, and IS001 binds within a groove around the active site in the same way FK866 does, except for the ribose ring. Most of the residues interacting with IS001 are involved in hydrophobic contacts, which are formed by Phe193(A), Arg196(A), Val242(A), Ala244(A), Ile309(A), Arg311(A), Arg349(A), Ile351(A), Asp354(A), Val378(A), Ser379(A), Asp16(B) and Tyr18(B) (Fig. 3). In particular, the pyridyl ring of IS001 is involved in π-π-stacking interactions with the side chains of Phe193(A) and Tyr18(B), as is observed in the FK866-complexed structure (Fig. 4A). Within the IS001-complexed structure, the hydrophobic part of IS001, which corresponds to FK866, is well ordered (average B factors of ~55 Å^2), while the added hydrophilic ribose ring is rather dynamic (average B factors of ~70 Å^2). Although our aim was to enable interactions between the ribose ring of IS001 and several hydrophilic residues in the visfatin binding site for NMN [Arg196(A), Arg311(A), Asp313(A), and Asp354(A)], we were unable to define the interactions around the ribose binding site. This may reflect a lack of contacts determining the exact orientation of the ribose ring of IS001 with respect to visfatin. Within the structure of the visfatin-NMN complex, the phosphate group of NMN is located in a highly hydrophilic binding pocket and interacts with a water molecule and the main-chain N atoms of Gly383 and Gly384. These contacts may affect the orientation of the ribose ring of NMN, enabling a tighter interaction with visfatin (Fig. 4B).

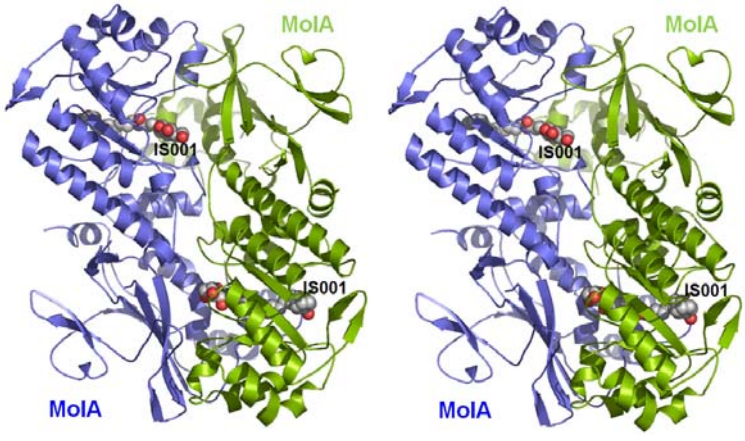

Fig. 2. Stereo diagram showing the visfatin dimer in complex with IS001. One monomer (MolA) is shown in blue, the other (MolB) in green. The bound IS001 molecules are shown as space-filling models.

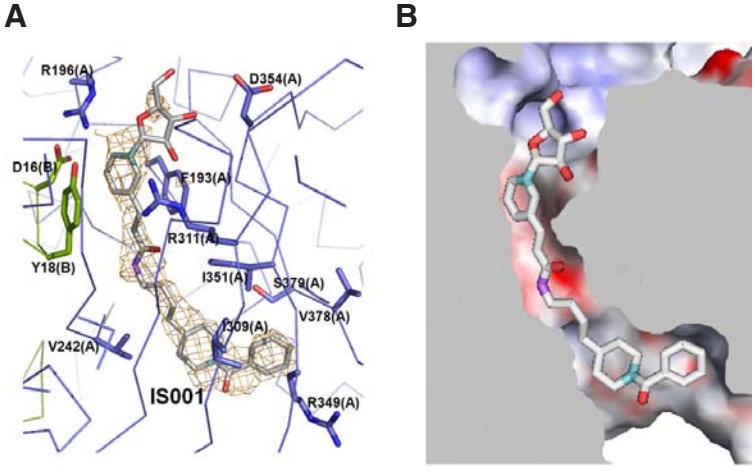

Fig. 3. The IS001 binding site on visfatin. (A) Close up view of the IS001 binding site on visfatin. The *2Fo-Fc* electron density map is contoured at 1 σ (orange mesh). (B) Surface representation of the IS001 binding site. IS001 (white) is shown as a ball and stick model. The electrostatic potential was calculated using APBS (Sanner et al., 1999). The potentials are colored from -21 kT (red) to +21 kT (blue).

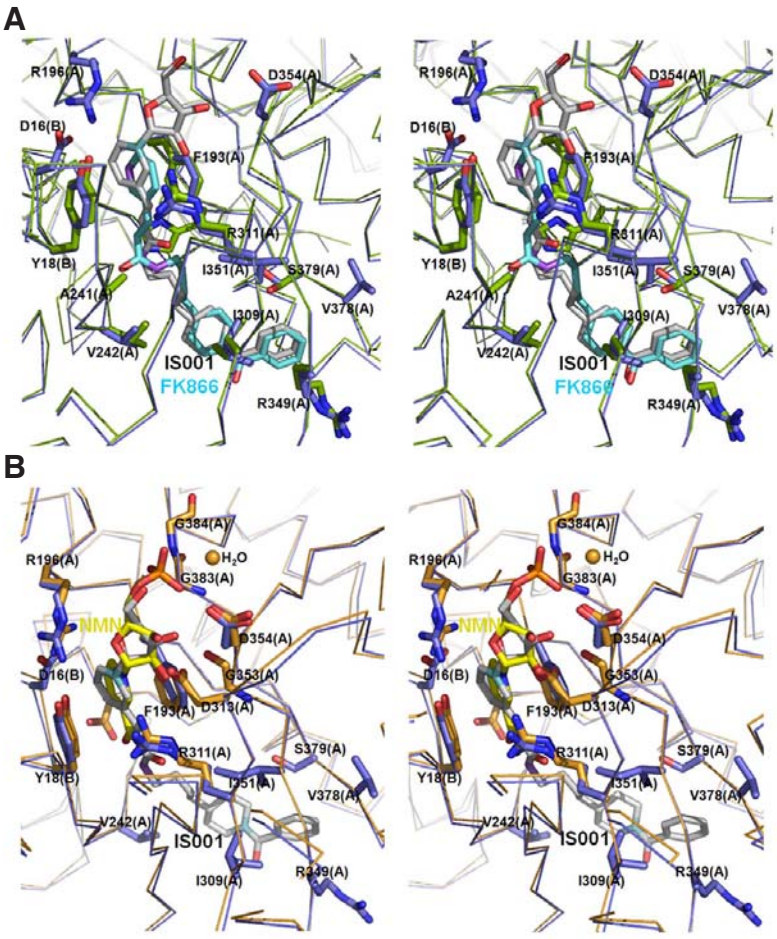

Fig. 4. Comparison of the binding site for IS001 with those for FK866 (A) and NMN (B). (A) Superimposition of the binding sites for IS001 and FK866 within the structures of visfatin-inhibitor complexes (PDB ID: 2G97). Residues mediating formation of the IS001-visfatin and FK866-visfatin complexes are shown in blue and green, respectively. IS001 (gray) and FK866 (cyan) are shown as ball and stick models. (B) Superimposition of the respective binding sites within the structures of the IS001- visfatin and NMN-visfatin (PDB ID: 2G96) complexes. Residues mediating the formation of IS001-visfatin and NMN-visfatin are shown in blue and orange, respectively. IS001 (gray) and NMN (yellow) are shown as ball and stick models.

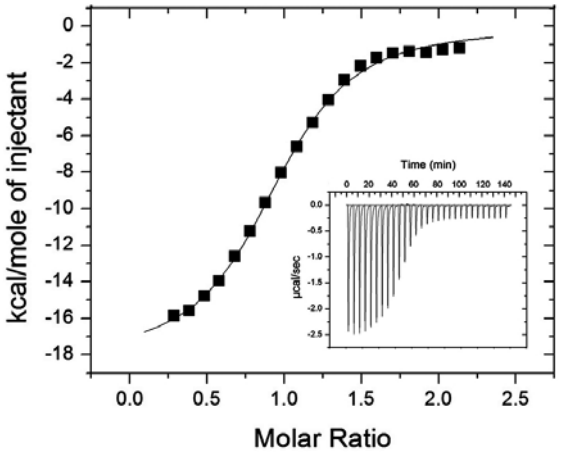

Fig. 5. Calorimetric titration of visfatin with IS001. The black squares depict the isothermal titration calorimetric binding curve for visfatin titrated with IS001. The fit is shown as a thin line [The K_d is $4.5 \pm 0.28 \times 10^{-6}$ M].

We also measured the affinity of IS001 for visfatin using ITC. Consistent with its higher B-factor, IS001 had a lower affinity for visfatin ($K_d = 4.5 \pm 0.28 \times 10^{-6}$ M) than FK866 (on the order of 10^{-9} M) (Fig. 5). Non-polar residues make up about 85% of the interface between visfatin and FK866, which form the hydrophobic tunnel at the dimer interface. It is energetically unfavorable for the hydrophilic ribose of IS001 to pass through the hydrophobic tunnel of visfatin, which may result in the low affinity of visfatin for IS001. It also suggests that the polarity modulation on ribose ring will be necessary to minimize the unfavorable interactions.

We conclude that effective FK866-based inhibitor compounds must retain two major components: the pyridyl ring is needed to maintain π-π-stacking interactions with Phe193(A) and Tyr18(B), and the benzopiperidine group is needed to maintain the van der Waals interactions with about ten residues. Addition of a ribose ring to the pyridyl ring of FK866 did not improve its solubility and binding interactions, mainly because the ribose was not large enough to make hydrophilic contacts with visfatin's ribose binding residues, suggesting a bulkier modifying group will be needed to strengthen the interactions. Our studies provide structure-based insight into the design needed for optimization of visfatin inhibitors.

ACKNOWLEDGMENTS

We thank Drs. Heung-Soo Lee, Kyung-Hwa Kim, Kyung Jin Kim, and Yeon-Gil Kim of BL-4A at the Pohang Accelerator Laboratory, Pohang, Korea, for their kind support during data collection. This work was supported by a grant from the Korea Healthcare Technology Research and Development Project, Ministry for Health, Welfare and Family Affairs, Republic of Korea (A062442).

REFERENCES

Brunger, A.T., Adams, P.D., Clore, G.M., and DeLano, W.L. (1998). Crystallography & NMR system: A new software suite for macromolecular structure determination. Acta Cryst. D. *54*, 905-921.

Burkle, A. (2005). Poly(ADP-ribose): The most elaborate metabolite of NAD^+. FEBS J. *272*, 4576-4589.

Drevs, J., Loser, R., Rattel, B., and Esser, N. (2003). Antiangiogenic potency of FK866/K22.175, a new inhibitor of intracellular NAD biosynthesis, in murine renal cell carcinoma. Anticancer Res. *23*, 4853-4858.

Emsley, P., and Cowtan, K. (2004). Coot: model-building tools for molecular graphics. Acta Cryst. D. *60*, 2126-2132.

Hasmann, M., and Shcemainda, I. (2003). FK866, a highly specific noncompetitive inhibitor of nicotinamide phosphoribosyltransferase, represents a novel mechanism for induction of tumor cell apoptosis. Cancer Res. *63*, 7436-7442.

Holen, K., Saltz, L.B., Hollywood, E., Burk, K., and Hauske, A.R. (2008). The pharmacokinetics, toxicities, and biologic effects of FK866, a nicotinamide adenine dinucleotide biosynthesis inhibitor. Invest. New Drugs *26*, 45-51.

Hufton, S.E., Moerkerk, P.T., Brandwijk, R., de Bruïne, A.P., Arends, J.W., and Hoogenboom, H.R. (1999). A profile of differentially expressed genes in primary colorectal cancer using suppression subtractive hybridization. FEBS Lett. *463*, 77-82.

Khan, J.A., Tao, X., and Tong, L. (2006). Molecular basis for the inhibition of human visfatin, a novel target for anticancer agents. Nat. Struct. Mol. Biol. *13*, 582-586.

Kim, M.K., Lee, J.H., Kim, H., Park, S.J., Kim, S.H., Kang, G.B., Lee, Y.S., Kim, J.B., Kim, K.K., Suh, S.W., et al. (2006). Crystal structure of visfatin/pre-B cell colony enhancing factor 1/nicotinamide phosphoribosyltransferase, free and in complex with the anticancer agent FK-866. J. Mol. Biol. *362*, 66-77.

Laskowski, R.A., MacArthur, M.W., Moss, D.S., and Thornton, J.M. (1993). PROCHECK: a program to check the stereochemical quality of protein structures. J. Appl. Cryst. *26*, 283-291.

Otwinowski, Z., and Minor, W. (1997). Processing of X-ray diffraction data collected in oscillation mode. Methods Enzymol. *276*, 307-326.

Sanner, M.F. (1999). Python: a programming language for software integration and development. J. Mol. Graphics Mod. *17*, 57-61.

Schreiber, V., Dantzer, F., Ame, J.C., and de Murcia, G. (2006). Poly(ADP-ribose): novel functions for an old molecule. Nat. Rev. Mol. Cell. Biol. *7*, 517-528.

Vagin, A., and Teplyakov, A. (2000). An approach to multi-copy search in molecular replacement. Acta Cryst. D. *56*, 1622-1624.

Van Beijnum, J.R., Moerkerk, P.T., Gerbers, A.J., De Bruïne, A.P., Arends, J.W., Hoogenboom, H.R., and Hufton, S.E. (2002). Target validation for genomics using peptide-specific phage antibodies: a study of five gene products overexpressed in colorectal cancer. Int. J. Cancer *101*, 118-127.

Wang, T., Zhang, X., Bheda, P., Revollo, J.R., Imai, S., and Wolberger, C. (2006). Structure of Nampt/PBEF/visfatin, a mammalian NAD+ biosynthetic enzyme. Nat. Struct. Mol. Biol. *13*, 661-662.

Won, J., Chung, S.Y., Kim, S.B., Byun, B.H., Yoon, Y.S., and Joe, C.O. (2006). Dose-dependent UV stabilization of p53 in cultured human cells undergoing apoptosis is mediated by poly(ADP-ribosyl)ation. Mol. Cells *21*, 218-223.

Wosikowski, K., Mattern, K., Schemainda, I., Hasmann, M., Rattel, B., and Löser, R. (2002). WK175, a novel antitumor agent, decreases the intracellular nicotinamide adenine dinucleotide concentration and induces the apoptotic cascade in human leukemia cells. Cancer Res. *62*, 1057-1062.

Ziegler, M. (2000). New functions of a long-known molecule. Eur. J. Biochem. *267*, 1550-1564.